Semi-AI Approach for RSRP Prediction with Closed-Form Coverage Preservation in Cellular Networks

Passawee Sombunwanich
School of Engineering, King Mongkut's Institute of Technology Ladkrabang
Bangkok, Thailand
67016148@kmitl.ac.th

Watid Phakphisut
School of Engineering, King Mongkut's Institute of Technology Ladkrabang
Bangkok, Thailand
watid.ph@kmitl.ac.th

Tanun Jaruvitayakovit
Advanced Wireless Network Company Limited
Bangkok, Thailand
tanunjar@ais.co.th

***Abstract*—Accurate Reference Signal Received Power (RSRP) prediction is essential for wireless network planning and optimization. Traditional methods rely on drive test data, which are costly and spatially limited. Several studies have presented AI-driven approaches using measurement reports (MRs) from user equipment (UE). These deep neural network (DNNs) were trained using MR and cell configuration data, outperforming the standard propagation model (SPM). However, lightweight models trained using MR data exhibit distortion in coverage due to the limited data in certain areas. To address this, we propose Semi-AI, a transfer learning-based framework that fine-tunes trained models to align predictions with real-world signals. In contrast to typical transfer learning applications, which aim to reduce training time, Semi-AI seeks to preserve the signal coverage generated by the path loss model, maintain high prediction accuracy, and offer flexible coverage planning without extensive drive testing.**

***Index Terms*—Reference Signal Received Power, Transfer Learning, Cellular Network, Deep Learning.**

I. Introduction

In modern wireless communication networks, accurately predicting the Reference Signal Received Power (RSRP) is crucial for network planning and optimization, enhancing both coverage and performance. Conventional approaches to path loss modeling typically rely on empirical data obtained through drive tests. The collected measurements are fitted to a Standard Propagation Model (SPM) [1], which estimates path loss and consequently calculate RSRP for each area. However, drive tests incur substantial operational costs, especially when conducted over large geographical regions. Furthermore, such tests are inherently limited in spatial resolution, as measurements are primarily confined to roadways and may not accurately represent all user locations. An alternative methodology involves using Measurement Report (MR) data obtained from user equipment (UE) at various positions. These MR data, sourced by mobile network operators (MNOs), reflect real-world signal conditions but may contain measurement noise due to device heterogeneity. MR data exist in two formats: one records only the strongest RSRP of the serving cell in each grid, referred to as the dominant grid; the other records all received RSRP from various cells, referred to as the non-dominant grid. However, non-dominant grid data require substantially greater storage capacity—for example, recording top five strongest RSRPs consumes more than 2.18 times the storage used by dominant grid data.

Several studies have proposed machine learning techniques for RSRP prediction. For example, the study using the drive test dataset in Putrajaya Malaysia, conducted by [2], employed a random forest model to predict RSRP, achieving a root mean square error (RMSE) of 5.74 dB. The study in Denmark [3] used a drive test dataset in combination with satellite images and a path loss model within a convolutional neural network (CNN) to predict path loss, achieving RMSEs of 4.4 dB and 4.2 dB at 811 MHz and 2630 MHz, respectively. In another study [4], RSRP prediction in China utilized physical features such as link distance, base station height and geospatial data (e.g., clutter index, altitude, and building height). This approach achieved an RMSE of 5.12 dB using a CNN model. Similarly, the study in the Bangkok Metropolitan Area (BMA), Thailand [5], employed CNN models incorporating geospatial data and antenna configuration, achieving an RMSE of 2.92 dB. These studies demonstrate high accuracy in RSRP prediction.

In this study, to address potential training challenges associated with newly collected data, the RSRP prediction results are reproduced using a lightweight deep neural network (DNN) architecture trained on MR data. Newly available data can subsequently be used to retrain or fine-tune the model prior to prediction. Inputs to the lightweight model include MR data and cell configuration parameters, provided by the MNO. For dominant grid, the lightweight model achieves an RMSE of 4.041 dB, representing a significant improvement over the SPM, which yields an RMSE of 11.630 dB. Although our model does not outperform those presented in studies [3] - [5], it is considerably more lightweight and requires significantly fewer input features. Moreover, in this work, we highlight a critical limitation encountered when using MR data to train lightweight model. It exhibits a noticeable distortion in the predicted coverage area, as illustrated in Fig. 1a. This distortion likely results from the inherent incompleteness of

the MR dataset. Specifically, UEs typically do not report RSRP values in areas where signal strength is extremely poor or falls below a certain threshold. Consequently, the training data lack representation of the weak-signal, far-edge, or non-coverage regions. As the lightweight model learns only from the available, mostly good-to-moderate signal data, its prediction inherently extrapolates from a biased sample, leading to inaccurate coverage. Furthermore, this deficiency renders the lightweight model unsuitable for radio network optimization tasks, such as antenna parameter tuning. Even when the antenna model is changed (as illustrated by comparing Fig. 1a and Fig. 1b), the predicted coverage continues to exhibit this distortion, masking the true impact of the optimization.

To address the aforementioned limitation, we propose a lightweight model based on transfer learning (TL). TL has been widely recognized for its ability to reduce training time and computational overhead, particularly in large-scale applications such as CNNs and natural language processing. However, in this study, TL is not employed primarily for computational efficiency. Instead, it is leveraged to maintain consistency with signal coverage generated by analytical path loss models during RSRP prediction. This model is referred to as the semi-AI model. By fine-tuning a pre-trained model, an RMSE of 5.955 dB is achieved while preserving the coverage generated by the SPM, as demonstrated in Fig. 1c. Crucially, the semi-AI model retains its ability to accurately reflect the impact of changes in the antenna model as shown in Fig. 1d, making it suitable for subsequent radio network optimization tasks.

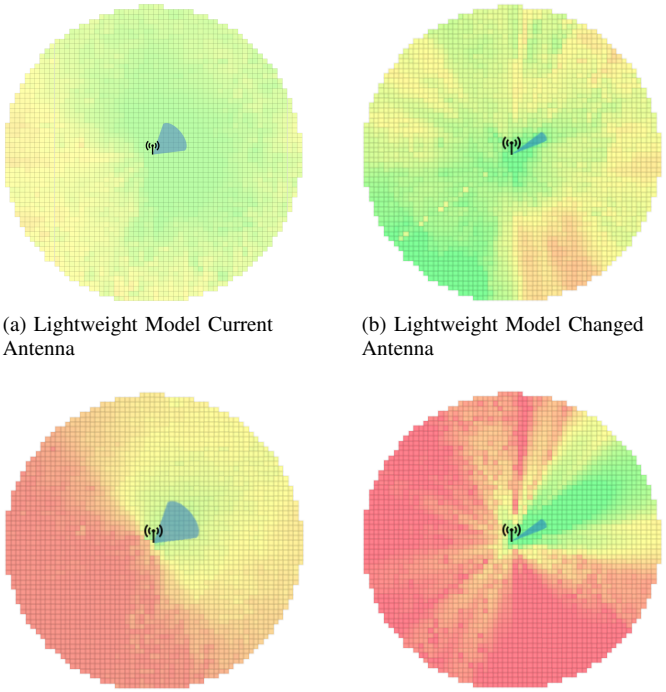

(a) Lightweight Model Current Antenna

(b) Lightweight Model Changed Antenna

(c) Semi-AI Model Current Antenna

(d) Semi-AI Model Changed Antenna

Fig. 1. Coverage prediction results comparing the lightweight model ((a) and (b)) and the Semi-AI model ((c) and (d)). The prediction is shown for two antenna configurations: the Current Antenna (wider HPBW, (a) and (c)) and a Changed Antenna (narrower HPBW, (b) and (d)).

II. Parameters

The data used in this study comprise MR, cell configuration data, and open-source geospatial data. This study utilizes two datasets collected from the 1800 MHz LTE network. The first dataset, in dominant grid format, was collected in BMA, Thailand, on 4 September 2024. The second dataset, in non-dominant grid format, was collected in Bangkok, Thailand, on 2 September 2024. Both datasets were provided by Advanced Wireless Network Company Limited. The dominant grid dataset includes approximately a million grid points, 6,000 eNodeB IDs, and 18,000 cell IDs, spanning an area of roughly 7,761 km^2 within the BMA. The non-dominant grid includes approximately one million grid points, 3,800 eNodeB IDs, and 10,700 cell IDs, covering an area of roughly 1,568 km^2 within Bangkok. The parameters utilized in this analysis are summarized in Table I.

A. Measurement Report

The MR data consist of the daily average of signal measurement—i.e., RSRP—along with the associated serving cell and the fixed position of the UE within a 50 m $\times$ 50 m grid. The MR data are available in two formats: dominant and non-dominant grid.

In this work, the non-dominant grid format records the five strongest RSRP values per grid point from various cells, as shown in Fig. 2a, while the dominant grid format records only the best-serving cell for each grid point—i.e., the cell with the strongest RSRP—as shown in Fig. 2b. The dominant grid format is more storage-efficient, requiring approximately 2.18 times less space than the non-dominant grid format, based on a comparison over a 1,568 km^2 area.

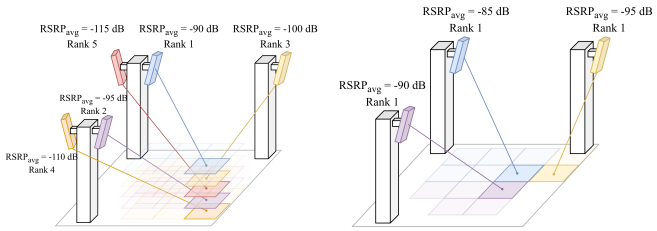

(a) Non-dominant grid.

(b) Dominant grid.

Fig. 2. MR data formats.

B. Cell Configuration

The cell configuration dataset contains a set of parameters characterizing the operational and physical attributes of each LTE cell. These include the operating frequency band, reference signal power (P_B), physical azimuth—i.e., horizontal direction from geographic north (ϕ_P), mechanical tilt (θ_m), electrical tilt (θ_e), antenna gain (G_{ant}), horizontal beamwidth (HBW), and antenna model. The dataset also provides the height from the ground to the antenna installation point (h_B).

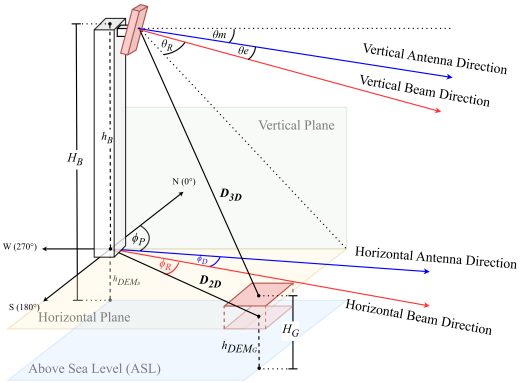

Fig. 3. Example parameters of lightweight model.

However, in this work, a digital elevation model (DEM) sourced from [6] is used to compute the antenna and UE heights, denoted as H_B and H_G, respectively.

C. Standard Propagation Model (SPM)

The well-known SPM [1] is suitable for predictions in the 150–3500 MHz frequency band over distances ranging from 1–20 km. The SPM is calibrated using measured path loss data, which is calculated by

$$\begin{aligned} PL_{SPM} = {} & K_1 + K_2 \log(D_{2D}) + K_3 \log(H_B) \\ & + K_4 \cdot D_{loss} + K_5 \log(D_{2D}) \log(H_B) \\ & + K_6 H_G + K_7 \log(H_G) \\ & + K_{clutter} f_{clutter} + K_{hill} \ , \end{aligned} \tag{1}$$

where D_{2D} is 2D distance between antenna and UE; K_1 is constant offset (dB); K_2, K_3, K_4, K_5, K_6, and K_7 are multiplying factors; D_{loss} represents losses due to diffraction over obstructed paths (dB); $f_{clutter}$ denotes average clutter-related losses;$K_{clutter}$ is the corresponding multiplying factor; and K_{hill} is corrective factor for hilly regions.

In this study, MR data are used to calibrate the SPM. However, due to the impracticality of obtaining certain measurements across large operational area, the parameters D_{loss}, $f_{clutter}$, and K_{hill} are excluded from the calibration process. Consequently, the final SPM equation becomes

$$\begin{aligned} PL_{SPM} = {} & K_1 + K_2 \log(D_{2D}) + K_3 \log(H_B) \\ & + K_4 \log(D_{2D}) \log(H_B) \\ & + K_5 H_G + K_6 \log(H_G) \ . \end{aligned} \tag{2}$$

III. Semi-AI

A. Lightweight Model for RSRP prediction

In this work, the proposed lightweight model is designed to predict the path loss error (PL_{Error}), aiming to compensate for the incompleteness of SPM. Subsequently, the RSRP is calculated as

$$RSRP = P_B + G_B^{3D} - (PL_{SPM} + PL_{Error}) \ , \tag{3}$$

TABLE I
Given Parameters

Type	Parameter	Definition
Measurement Report	lat_G, lng_G	Latitude and longitude of UE
	$RSRP$	Reference signal received power (dBm)
Cell Configuration	lat_B, lng_B	Latitude and longitude of eNodeB
	h_B	Height from the ground to antenna (m)
	ϕ_P	Azimuth angle of antenna direction (deg.)
	ϕ_D	Angle from antenna direction to horizontal beam direction (deg.)
	θ_m, θ_e	Antenna mechanical and electrical tilt (deg.)
	G_{ant}	Antenna Gain (dBi)
	P_B	Reference signal power (dBm)
	HBW	Horizontal beam width of antenna (deg.)
Open Source Data	h_{DEM}	Digital elevation model (m)

TABLE II
Input Parameters

Parameter	Obtained from
lat_B, lng_B	Table I
θ_m, θ_e	Table I
θ_{tilt}	Equation (5)
$\cos\phi_R$, $\sin\phi_R$	Fig. 3
$\cos\theta_R$, $\sin\theta_R$	Fig. 3
$\cos\phi_P$, $\sin\phi_P$	Table I
$\cos\phi_{MB}$, $\sin\phi_{MB}$	Equation (6)
$\cos\phi_G$, $\sin\phi_G$	Equation (7)
D_{2D}, D_{3D}	Fig. 3
H_B, H_G	Fig. 3
H_r	Equation (4)
HBW	Table I
P_B	Table I
G_{ant}	Table I
G_B^{3D}	Ref. [7]
PL_{SPM}	Equation (2)

where G_B^{3D} is an antenna gain computed using a three-dimensional directive antenna pattern interpolation method [7].

The architecture of the lightweight model comprises nine hidden layers, as shown in Fig. 4. The first four layers employ the hyperbolic tangent (tanh) activation function, while the remaining five layers utilize the Gaussian Error Linear Unit (GELU) activation function. As shown in Table II, a total of 25 input parameters are used in the lightweight model. For example, the 2D distance (D_{2D}) and 3D distance (D_{3D}) from the antenna to the grid point, illustrated in Fig. 3, are included. Additionally, the height ratio between the transmitter

and receiver (H_r), is calculated as

$$H_r = H_B / H_G \ . \tag{4}$$

Furthermore, derived parameters—i.e., the total antenna tilt (θ_{tilt}), the beam azimuth of the transmitting cell (ϕ_{MB}), and the azimuth from the transmitting cell to each grid point (ϕ_G)—are also used, as proposed in [4], and are formulated by

$$\theta_{tilt} = \theta_m + \theta_e \ , \tag{5}$$

$$\phi_{MB} = \phi_P + \phi_D \ , \tag{6}$$

$$\phi_G = \phi_{MB} + \phi_R \ . \tag{7}$$

B. Constructing Semi-AI Model Through Transfer Learning

TL is frequently employed to reduce training time and computational complexity. In this study, however, it is used to preserve the signal coverage characteristics generated by SPM, while enabling the model to learn the path loss error from the MR data. The model construction consists of a training phase and a tuning phase. First, the lightweight model is trained using synthetic data generated by SPM, augmented with Gaussian noise, as shown in Fig. 8b and Fig. 9b. The synthetic data are generated using various antenna models and parameter variations —i.e., ϕ_P, θ_m and θ_e. The training process is illustrated in Fig. 6.

After training, all layers are frozen except for the first and last layers, which are indicated as colored layers in Fig. 5. The model is then tuned using the MR corresponding to the target cell ID. The tuning process is depicted in Fig. 7. This tuning allows the unfrozen layers to adaptively learn the path loss error specific to each cell ID, while the frozen layers preserve the coverage representation learned from the synthetic data. The tuning process enables the model to replicate the path loss characteristics of each cell ID in a manner similar to SPM, while leveraging the learning capability to reduce prediction error. A significant advantage of this architecture is its ability to continuously adapt to changes in the radio environment; by simply fine-tuning the unfrozen layers using the newly available data, the semi-AI model can be quickly updated to reflect the most current propagation conditions and network deployment status.

IV. Results

To evaluate the performance of the models, two distinct metrics are utilized. The first metric is the RMSE, which quantifies the statistical discrepancy between the measured and predicted RSRP values, which is formulated as

$$RMSE = \sqrt{\frac{1}{n_{sample}} \sum_{i=1}^{n_{sample}} \left(y_i - \widehat{y_i}\right)^2} \ , \tag{8}$$

where n_{sample} is number of grid points, y_i is the measured RSRP value, and $\widehat{y_i}$ is predicted RSRP value.

The second metric, the Propagation Model Consistency Error (PMCE), is introduced to evaluate the fidelity of the predicted coverage relative to the expected coverage by the analytical path loss model. The PMCE specifically measures the discrepancy between the predicted RSRP values and the RSRP values generated by the SPM. This metric is crucial for assessing how well a model can adapt to new antenna configurations without inheriting the coverage bias present in the historical MR data.

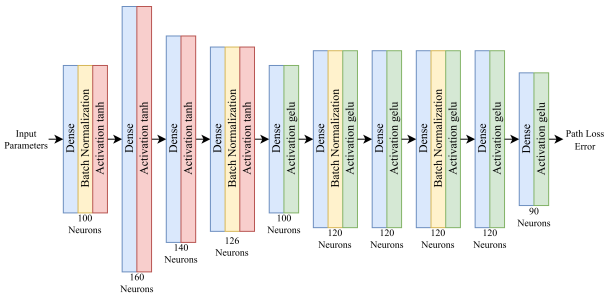

Fig. 4. Lightweight model for RSRP prediction.

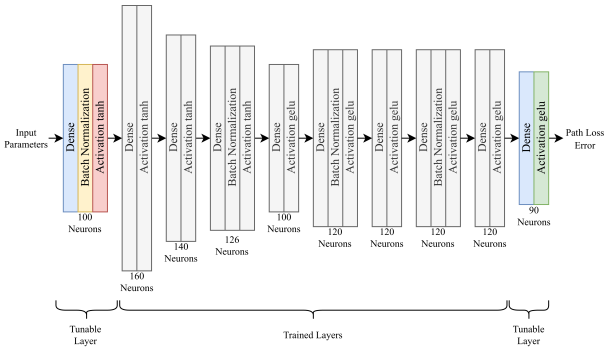

Fig. 5. Trained and tunable layers of semi-AI.

$$PMCE = \sqrt{\frac{1}{n_{sample}} \sum_{i=1}^{n_{sample}} \left(y_i^{SPM} - \widehat{y_i}\right)^2} \ , \tag{9}$$

where y_i^{SPM} is the RSRP value generated by the SPM at grid i, and $\widehat{y_i}$ is the predicted RSRP value. A lower PMCE indicates that the predicted coverage aligns more closely with the theoretical coverage generated by the SPM.

The SPM and Semi-AI models are trained and evaluated on a per-cell ID basis, while the lightweight model is trained using a dataset encompassing all cell IDs. To ensure fair comparison, weighted average RMSE and PMCE values are computed, accounting for the differing number of grid points per cell, as calculated by

$$\overline{RMSE} \text{ or } \overline{PMCE} = \frac{\sum_{j=1}^{n_{cell}} n_{sample_j} \cdot \text{Metric}_j}{\sum_{j=1}^{n_{cell}} n_{sample_j}} \ , \tag{10}$$

where n_{cell} is number of cell IDs and Metric_j represents either $RMSE_j$ or $PMCE_j$.

The model evaluation results are presented in Fig. 10 and Fig. 11. The dominant grid dataset comprises approximately 1 million grid points across 7,781 km^2 in BMA, while the non-dominant grid covers roughly 1 million grid points across

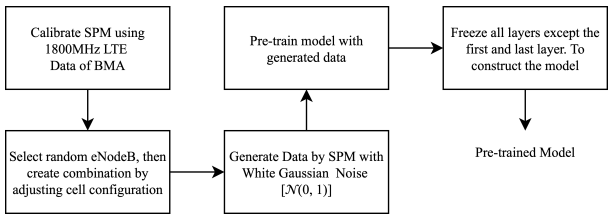

Fig. 6. Training process of semi-AI.

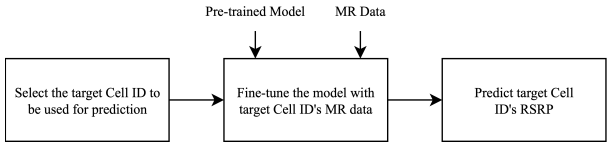

Fig. 7. Tuning process of semi-AI.

1,568 km^2 in Bangkok. Examples of dominant and non-dominant grid are shown in Fig. 8a and Fig. 9a, corresponding to cell ID-1 on eNodeB-A.

In the dominant grid dataset, the SPM exhibits RMSE values of 6.448 dB (training) and 11.630 dB (testing), indicating a significant generalization gap and poor alignment with measured RSRP values. In contrast, the lightweight model achieves substantially lower RMSE values of 3.483 dB (training) and 4.041 dB (testing). However, the lightweight model's PMCE is significantly higher, at 25.174 dB, confirming that although it fits historical MR data well, it produces distorted coverage predictions lacking alignment with the expected coverage (see Fig. 8c).

The Semi-AI model, fine-tuned for 2000 epochs, effectively mitigates the coverage distortion, as shown in Fig. 8d-8i. It achieves RMSE values of 4.918 dB (training) and 5.415 dB (testing), while significantly reducing the PMCE to 7.134 dB. This indicates that the semi-AI model effectively preserves the theoretical coverage generated by the SPM while improving prediction accuracy. Based on this performance, the semi-AI model trained for 2000 epochs is selected as the preferred model for coverage prediction and network optimization.

Further evaluation on the non-dominant grid confirms these performance characteristics. The SPM yields RMSE values of 8.585 dB (training) and 10.510 dB (testing). The lightweight model again achieves low RMSE values of 4.918 dB (training) and 5.415 dB (testing), but a high PMCE of 24.196 dB, indicating a persistent issue with distorted coverage. In contrast, the Semi-AI model achieves RMSE values of 4.844 dB (training) and 7.674 dB (testing), with a much lower PMCE of 9.881 dB. This demonstrates that the semi-AI model maintains fidelity to the SPM-generated coverage while improving prediction accuracy, making it suitable for real-world planning and optimization tasks.

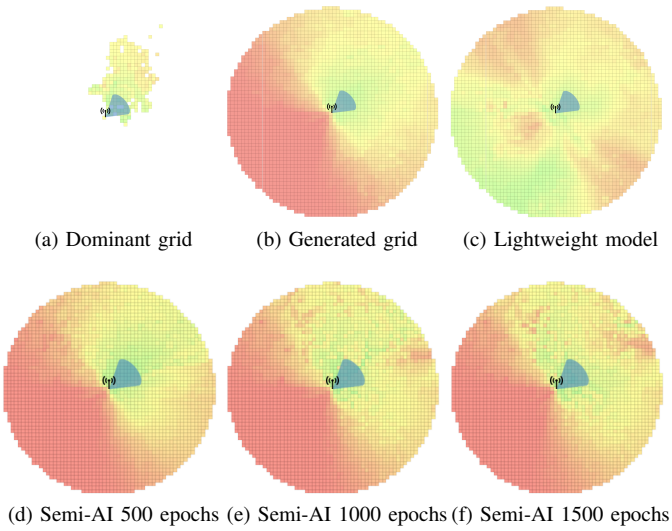

(a) Dominant grid (b) Generated grid (c) Lightweight model

(d) Semi-AI 500 epochs (e) Semi-AI 1000 epochs (f) Semi-AI 1500 epochs

(g) Semi-AI 2000 epochs (h) Semi-AI 2500 epochs (i) Semi-AI 3000 epochs

Fig. 8. Coverage prediction of dominant grid model.

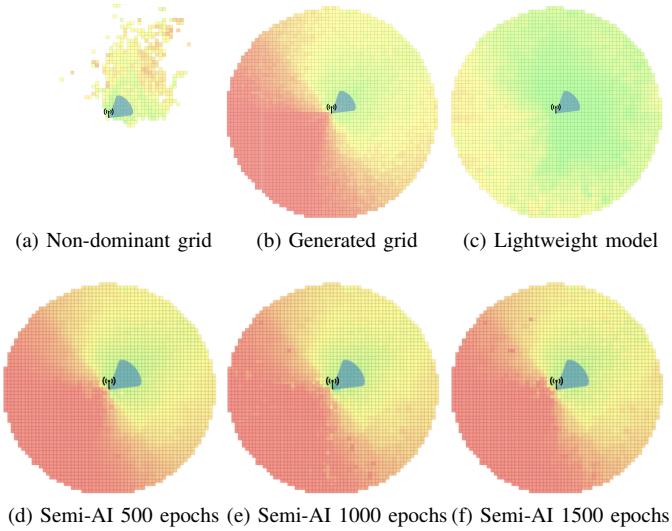

(a) Non-dominant grid (b) Generated grid (c) Lightweight model

(d) Semi-AI 500 epochs (e) Semi-AI 1000 epochs (f) Semi-AI 1500 epochs

(g) Semi-AI 2000 epochs (h) Semi-AI 2500 epochs (i) Semi-AI 3000 epochs

Fig. 9. Coverage prediction of non-dominant grid model.

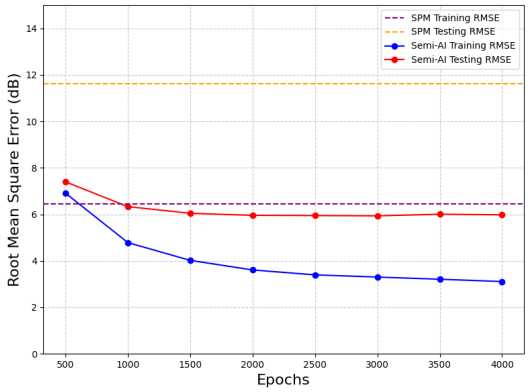

Fig. 10. Semi-AI performance on dominant grid.

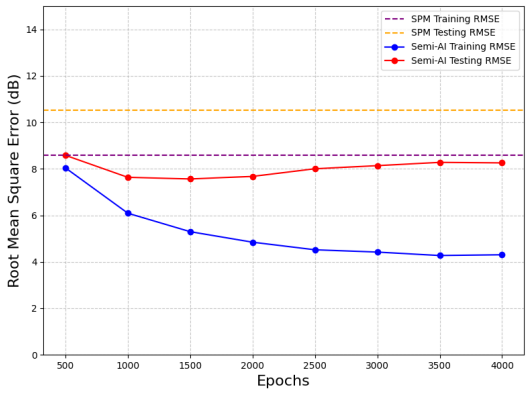

Fig. 11. Semi-AI performance on non-dominant grid.

V. Conclusion

This study proposed a semi-AI model to address the critical coverage distortion problem inherent in lightweight model trained using MR data. Quantitatively, the semi-AI model achieved high predictive accuracy on both dominant and non-dominant datasets, significantly outperforming the SPM—for example, achieving an RMSE of 5.955 dB compared to 11.630 dB on the dominant grid. Crucially, by minimizing the PMCE, the semi-AI model successfully mitigated the distortion and preserved the fidelity of the analytical coverage. This improved consistency demonstrates the suitability of the proposed semi-AI model for reliable RSRP prediction and subsequent radio network optimization tasks. With the added benefit that its fine-tuning mechanism allows for rapid and continuous adaptation to the newly available data.

Acknowledgment

This study was supported in part by the Program Management Unit for Competitiveness Enhancement (PMUC) and Advanced Wireless Network Company Limited.

TABLE III
RMSE Performance Comparison

Data format	Model	RMSE (dB)		Coverage
		Training	Testing	
Dominant Grid	SPM	6.448	11.630	Preserved
	Lightweight model	3.483	4.041	Distorted
	Semi-AI 2000 epochs	3.751	5.955	Preserved
Non-Dominant Grid	SPM	8.585	10.510	Preserved
	Lightweight model	4.918	5.415	Distorted
	Semi-AI 2000 epochs	4.844	7.674	Preserved

TABLE IV
PMCE for Coverage Fidelity Assessment

Trained dataset	Model	PMCE (dB)
Dominant Grid	Lightweight model	25.174
	Semi-AI 1000 epochs	6.803
	Semi-AI 2000 epochs	7.134
	Semi-AI 3000 epochs	7.220
	Semi-AI 4000 epochs	7.374
Non-Dominant Grid	Lightweight model	24.196
	Semi-AI 1000 epochs	9.284
	Semi-AI 2000 epochs	9.881
	Semi-AI 3000 epochs	10.306
	Semi-AI 4000 epochs	10.599

References

[1] *ATOLL 3.2.0 Model Calibration Guide*, Forsk, France, release: AT_320_MCG_E2. Online access: www.forsk.com.
[2] M. F. Ahmad Fauzi, R. Nordin, N. F. Abdullah, and H. A. H. Alobaidy, "Mobile network coverage prediction based on supervised machine learning algorithms," *IEEE Access*, vol. 10, pp. 55 782–55 793, 2022.
[3] J. Thrane, D. Zibar, and H. L. Christiansen, "Model-aided deep learning method for path loss prediction in mobile communication systems at 2.6 ghz," *IEEE Access*, vol. 8, pp. 7925–7936, 2020.
[4] Z. Yi, L. Zhiwen, H. Rong, W. Ji, X. Wenwu, and L. Shouyin, "Feature extraction in reference signal received power prediction based on convolution neural networks," *IEEE Communications Letters*, vol. 25, no. 6, pp. 1751–1755, 2021.
[5] T. Wongphatcharatham, W. Phakphisut, T. Jaruvitayakovit, A. Boonkajay, and J. Huang, "Deep learning aided robust rsrp prediction in cellular networks," in *2024 IEEE 100th Vehicular Technology Conference (VTC2024-Fall)*, 2024, pp. 1–5.
[6] H. Duester, "SRTM-Downloader," https://github.com/hdus/SRTM-Down.
[7] N. R. Leonor, R. F. S. Caldeirinha, M. G. Sánchez, and T. R. Fernandes, "A three-dimensional directive antenna pattern interpolation method," *IEEE Antennas and Wireless Propagation Letters*, vol. 15, pp. 881–884, 2016.